Experimental Identification of "Vacuum Heating" at Femtosecond-Laser-Irradiated Metal Surfaces

M. K. Grimes, A. R. Rundquist, Y.-S. Lee, and M. C. Downer*
Department of Physics, The University of Texas at Austin, Austin, Texas 78712
(Received 15 December 1998)

Aluminum and iron targets were irradiated by intense ($I \leq 10^{15}$ W/cm^2), 120 fs laser pulses with sufficiently high contrast such that the surface expanded no more than the peak electron quiver amplitude during excitation. Under these experimentally verified conditions, obliquely incident, p-polarized pulses uniquely experienced anomalous absorption, proportional to $(I\lambda^2)^{0.64}$, and as high as 20%. This extra absorption was distinguished from competing pump-induced linear mechanisms by fs-time-resolved reflectivity, and agreed quantitatively with essential features of Brunel's "vacuum heating," in which light is absorbed by drawing electrons into the vacuum and sending them back into the plasma with approximately the quiver velocity. [S0031-9007(99)09116-4]

PACS numbers: 52.50.Jm, 78.20.Ci, 78.47.+p

Amplified, high contrast femtosecond laser pulses [1] have opened a new regime of laser-solid interactions in which intense light is deposited into a solid faster than the target surface can hydrodynamically expand [2]. While numerous experiments have used a single pulse to both excite and probe such sharply bound solid density fluids [3], they have not individually identified the many competing collisional and collisionless absorption mechanisms unique to this regime which an extensive theoretical literature [4–10] has enumerated. For example, Brunel [4] proposed over ten years ago that a moderately intense, p-polarized light pulse incident obliquely on an atomically abrupt metal surface could be strongly absorbed by pulling electrons into the vacuum during an optical cycle, then returning them to the surface with approximately the quiver velocity. Later simulations [5] predicted that, with a slight surface expansion of scale length $L \equiv (\partial \ln n_e/\partial z)^{-1}$, the optical field would pull more electrons into the vacuum, and thus be even more strongly absorbed, as long as L did not significantly exceed the electron quiver amplitude $x_{\rm osc} = eE/m\omega^2$. While this "vacuum heating" (VH) mechanism has been incorporated into laser-plasma codes [6], and may influence surface x-ray [11] and high harmonic [12] generation, and intense laser interaction with nanoclusters [13] and hollow capillaries [14]—and although a microscopically similar mechanism underlies high harmonic generation and above-threshold ionization in gases [15]—quantitative experimental identification of VH at metal surfaces is completely lacking.

Two important barriers to such identification have been the production and verification of Brunel's condition $L \lesssim x_{\rm osc}$, and distinction of VH from competing linear mechanisms [7] such as inverse bremsstrahlung (IB), anomalous skin effect (ASE) [8], sheath inverse bremsstrahlung (SIB) [9], sheath transit absorption (STA) [10], and resonance absorption (RA) [16]. For example, 120 fs pulsed excitation at $\lambda = 0.62$ μm and peak intensity $I = 10^{15}$ W/cm^2 heats Al targets to a peak electron temperature of $kT_e \sim 100$ eV [3,7], resulting in a collision frequency $\nu \sim 5 \times 10^{15}$ s^{-1} [7]. For $L = 0$, IB dominates under these conditions [7] and is well described by the imaginary part ϵ_{0i} of the linear dielectric constant together with Fresnel's equations. ASE, SIB, and STA, which require collisionless transit of the skin depth $l_s \approx c/\omega_p \approx 100$ Å [i.e., $l_s \ll v_{\rm th}/\nu$, where $v_{\rm th} = (2kT_e/m)^{1/2}$], contribute very weakly since $l_s \sim 10 v_{\rm th}/\nu$ for the above conditions. Simulations by Andreev *et al.* confirm explicitly that ASE and SIB are negligible for the above pulse parameters [8]. On the other hand, Brunel predicted fractional VH absorption

$$f_{\rm VH} = (\eta/2\pi)(e/m\omega c\cos\theta)\frac{E_0^3}{E_L^2}, \qquad (1)$$

where E_L is the incident laser field, $E_0 = \xi E_L \sin\theta$ is the total incident + reflected field driving electron orbits normal to the surface, $1 < \xi < 2$ accounts for the complex reflectivity, and Brunel found numerically that $\eta = 1.75(1 + 2v_{\rm th}/v_{\rm osc})$ [4]. For the above conditions $f_{\rm VH} \approx 0.05$ at $\theta = 70°$. In principle, this absorption can be distinguished from competing linear mechanisms by its intrinsic I dependence $f_{\rm VH} \sim \sqrt{I\lambda^2}$, and its unique θ and polarization dependence. However, in single-pulse experiments variation of these laser parameters simultaneously changes the plasma conditions (kT_e, ionization state Z) on which linear absorption strongly depends, thus preventing identification of individual mechanisms. An uncharacterized expansion further obscures the situation by enhancing VH for $L \lesssim x_{\rm osc}$, and introducing RA for $L \gg x_{\rm osc}$. RA, like VH, requires obliquely incident p-polarized light, but unlike VH grows rapidly to a maximum by exciting a collective plasma oscillation at the critical surface ($\omega = \omega_p$) when $(\omega L_{\rm max}/c)^{1/3}\sin\theta \sim 0.8$ (typically, $L_{\rm max} \sim 0.1\lambda$) [16]. Although RA is linear for fixed L, it appears nonlinear (and thus harder to distinguish from VH) in self-reflectivity because of the intensity dependence of expansion velocity.

 0031-9007/99/82(20)/4010(4)$15.00

In this Letter, we report measurements in which the necessary condition ($L \lesssim x_{\rm osc}$) for VH absorption is satisfied and experimentally confirmed by twin-probe interferometry [17], and competing pump-induced linear absorption (RA, IB, ASE, SIB, STA) is separately characterized by conventional pump-probe reflectivity, thus rendering the predicted quantitative signatures of VH absorption clearly observable by I-, θ-, and polarization-dependent self-reflectivity. Polycrystalline Fe and Al targets were illuminated by 0.62 μm dye laser pulses with peak focused intensity $I \leq 10^{15}$ W/cm^2. Although our system could produce shorter, more intense pulses [18], optimum peak-to-pedestal contrast (10^5 at ± 0.9 ps and 10^3 at ± 0.23 ps)—and minimum target surface preexpansion—was achieved with the system operating at 120 fs and $I \leq 10^{15}$ W/cm^2 [19]. I (and thus $x_{\rm osc}$) was calibrated by standard pulse energy and spot size measurements and cross-checked by immersing the target surface in $\sim$1 atm He gas, which caused a sharp reflectivity drop and breakdown spark when $I \geq I_{\rm thresh} = 1.2 \pm 0.1 \times 10^{15}$ W/cm^2, the ionization threshold of He [20]. Since for $I < I_{\rm thresh}$, reflectivity was indistinguishable from separate measurements in vacuum and no nonspecular scatter was detected, we report results obtained in a He ambient. The sample was automatically translated after each laser shot to expose a fresh spot.

Target surface expansion and the combined effect of all *linear* pump-induced absorption mechanisms were characterized by (1) twin-probe interferometry [17] and (2) conventional pump-probe reflectivity, respectively, using a normally incident pump to avoid VH. In the former, the surface was probed by a pair of weak ($I < 10^{11}$ W/cm^2) collinear pulses whose frequency domain interference yields the phase shift $\Delta\phi$ acquired by the trailing probe on reflection from the excited surface. As an example, Fig. 1a shows $\Delta\phi_s(t)$ and $\Delta\phi_p(t)$ from the Fe surface excited at $I = 5.3 \times 10^{14}$ W/cm^2, probed at $\theta = 60°$ with an s- or p-polarized pulse pair, where t denotes the pump-trailing probe delay. For the latter measurement, one probe was blocked, and the delay t between the remaining probe and the pump was scanned, thus yielding conventional fs pump-probe reflectivity amplitudes $R_s(t)$ and $R_p(t)$, shown in Fig. 1b, under identical surface conditions. The four measured quantities $\Delta\phi_s(t)$, $\Delta\phi_p(t)$, $R_s(t)$, and $R_p(t)$, completely characterize the complex linear reflectance, and were fitted simultaneously to a model which includes (1) the time-varying dielectric constant $\epsilon_0(t) = \epsilon_{0r}(t) + i\epsilon_{0i}(t)$ at solid density, which implicitly describes the combined effect of pump-induced ionization, IB, ASE, SIB, and STA and (2) RA in the expanding density gradient of scale length $L(t)$, with density profile described by a Riemann solution of the surface hydrodynamic flow equations $n(z) = n_0[1 - z/4L(t)]^3$ [21], where fields within the sample were calculated by numerical solution of Helmholtz propagation equations [22]. For the short $L(\leq 0.02\lambda)$ of interest here, the fit

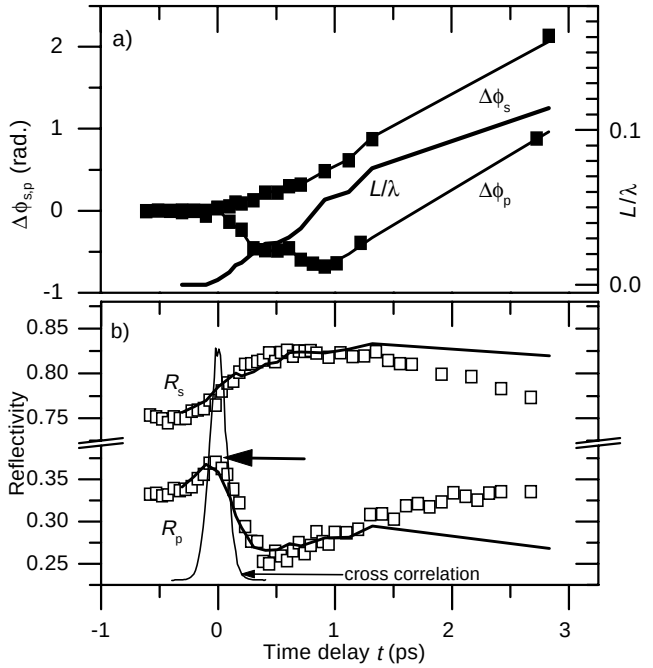

FIG. 1. Time resolved (a) phase shift and (b) reflectivity at s and p polarization for Fe at $\theta = 60°$, $I = 5.3 \times 10^{14}$ W/cm^2. Fit results from the density gradient model are also shown (lines). The density gradient scale length L/λ is shown with the right-hand axis.

was insensitive to the material-dependent functional dependence $\epsilon[n(z)]$ within the gradient [19]. The solid lines in Figs. 1a and 1b show the fit results, with the fitted $L(t)/\lambda$ shown in Fig. 1a. The agreement is excellent up to $t = 1$ ps, which corresponds to $L \simeq 0.06\lambda$. The fitted expansion velocity $4dL/dt = [2/(\gamma - 1)]\sqrt{ZkT_e/m_i} \sim 1.4 \times 10^7$ cm/s of the plasma-vacuum boundary [21] is consistent with the calculated [7] $kT_e \sim 100$ eV for these excitation conditions.

During the pump, L remains below 0.003λ, about equal to $x_{\rm osc}$ for 5.3×10^{14} W/cm^2, thus demonstrating that Brunel's criterion is achieved for an equivalent obliquely incident, p-polarized pump. This does not in itself prove the absence of residual RA. However, the simultaneously fitted $R_p(t)$ data in Fig. 1b *directly measure* RA, and show that RA is *negligible* ($<1\%$) during the pump. RA would decrease R_p, but, in fact, there is a slight *increase* in R_p (emphasized by an arrow) coincident with a rise in R_s which the model explains completely via changes in $\epsilon_0(t)$, which includes contributions from pump-induced ionization and non-RA linear absorption. After the pump, the sharp decrease in R_p coincides with expansion of the surface to $L \simeq 0.05\lambda$, and is indeed completely explained by RA. The quantitative accuracy with which the delayed absorption is explained by RA further supports the determination of negligible RA during the pump. This and similar results obtained for other I and targets demonstrate clearly that $L \lesssim x_{\rm osc}$ during the pump and that RA does not become important until after the pump.

To measure target absorption at large I for the *same* plasma conditions (T_e, Z, L) seen by the weak probes, we measured self-reflectivity of s- and p-polarized pulses for $10^{11} < I < 10^{15}$ W/cm^2 and incidence angles $20° \leq \theta \leq 70°$ varied in 5° increments. Representative results for $\theta = 20°$, 45°, and 65° are shown in Figs. 2a (Fe) and 2b (Al). An arrow highlights the Fe, $\theta = 65°$, p-polarized, $I = 5 \times 10^{14}$ W/cm^2 data in Fig. 2a, in order to contrast it directly with the low intensity, $\Delta t = 0$ probe reflectivity similarly highlighted in Fig. 1b, in which the probe was configured identically and the sample was pumped at the same I (i.e., driven to the same T_e, Z, L). The high I reflectivity is 20% *lower* than that of unpumped Fe, whereas the low I probe reflectivity was 10% *higher*. p-polarized absorption is thus *intrinsically* I dependent. The corresponding s-polarized reflectivities, on the other hand, are *identical* at low I (see Fig. 1b) and high I (see Fig. 2a). s-polarized absorption is thus intrinsically I independent (linear). The variation of s-polarized self-reflectivity with I evident throughout Fig. 2 is actually T_e and/or Z dependence, which is described by a linear dielectric constant. While p-polarized self-reflectivity also depends partly on T_e and Z, the intrinsically nonlinear component, illustrated by the contrast between weak probe and strong pulse reflectivity, signals the emergence of intrinsically I-dependent, p-polarized absorption possessing the basic properties of VH.

In order to define precisely the regime of intrinsically nonlinear absorption, the subset of data in Fig. 2 for which only linear absorption is expected (s-polarized for all I, θ; p-polarized for small I and/or θ) was fitted to Fresnel's equations using the linear dielectric constants $\epsilon_{0r}[I(T_e, Z)] + i\epsilon_{0i}[I(T_e, Z)]$ as fitting parameters at each I, yielding the dashed curves in Fig. 2 and the fitted dielectric constants shown in the inset of Fig. 3. These dielectric constants were then used to extrapolate the fit into the regime (p-polarized for large I, θ) of significant nonlinear absorption, also shown by the dashed curves. The divergence of the dashed curves from the large-I, p-polarized reflectivity data in Figs. 2a and 2b defines the magnitude of the "extra" nonlinear absorption. Note that, for the example highlighted by the arrow, the linear Fresnel fit correctly predicts the higher reflectivity of the weak p-polarized probe shown in Fig. 1b, and that the linear $\epsilon_{0r,0i}$ for Fe and Al converge to common values at high I, indicating that increasing ionization and heating

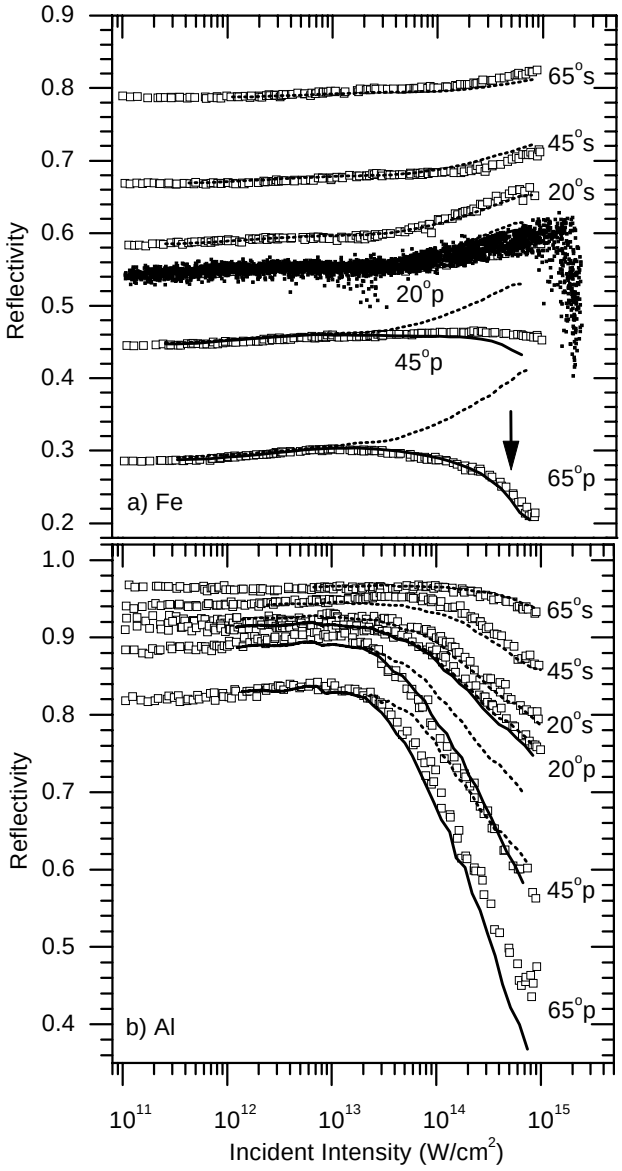

FIG. 2. Reflectivity vs intensity of (a) Fe and (b) Al at selected angles of incidence. Fresnel-only fit results are shown with dotted lines, and vacuum heating fit results with solid lines. The points are averages of 30 laser shots for all cases except p-polarized 20°, Fe, for which all shots are shown. For this case, the sharp reflectivity drop induced by ionization of He, which provides an intensity fiducial, is also shown.

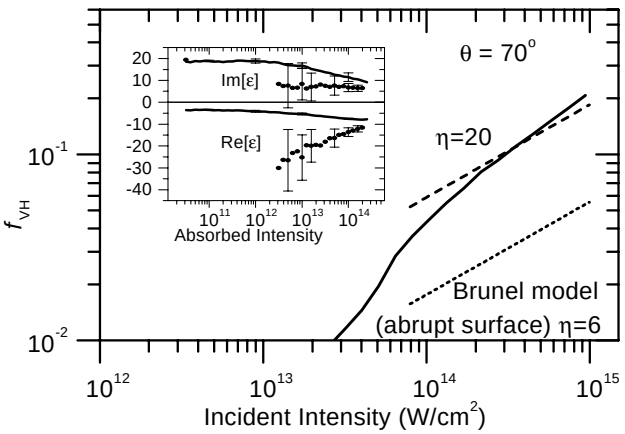

FIG. 3. Vacuum heating absorption fraction f_{VH} at $\theta = 70°$ from the best fit results to Fe data. The Brunel model prediction is also shown (dotted line) along with a simple scaling of the Brunel model to represent the effect of a nonzero gradient (dashed line). The top inset shows the dielectric constant resulting from the fit for Fe (lines) and Al (points).

create similar n_e and ν. Even though the background $\epsilon_{0r,0i}[I(T_e, Z)]$ evolve in completely different ways for each metal (Fig. 3, inset), the extra absorption increases in the same way for *both* metals as I and θ increase, in excellent agreement with Eq. (1). Thus the extra absorption is material independent, as expected for VH.

The absolute magnitude of the extra nonlinear absorption is plotted vs I in the main panel of Fig. 3 (solid curve) for $\theta = 70°$. For comparison, Brunel's idealized Eq. (1) describing f_{VH} for an *atomically abrupt* metal surface and a six-cycle pulse is plotted as a dotted line. This comparison brings out two key features of the measured absorption. First, the slope at 10^{15} W/cm^2 corresponds to a scaling $f_{\mathrm{VH}} \sim (I\lambda^2)^{0.64}$, in good agreement with the $\sqrt{I\lambda^2}$ dependence predicted by Eq. (1). Second, the measured absorption is a factor of 3 stronger than Brunel's idealized calculation, thus confirming the enhancement of VH predicted by particle simulations [5] for a slight gradient and a multicycle pulse because (1) the laser field penetrates further into the slightly graded surface, thus pulling more electrons into VH orbits; (2) electrons have a longer mean free path in the lower density gradient, further assisting their entry into collisionless VH orbits; and (3) VH orbital dynamics become increasingly chaotic with more cycles, which may also increase VH absorption. These inevitable features of realistic experiments can be parametrized by a single, best-fit, increased value of η in Eq. (1), yielding the upper dashed curve in Fig. 3 and, when added to linear absorption, the solid curves in Fig. 2, which agree excellently with *both* Fe and Al data for all θ and I, again highlighting the material independence of VH. Gibbon and Bell predict somewhat more complicated θ and I dependence, possibly because of the low density of the simulated ($n/n_{\mathrm{crit}} \sim 2$) compared to the actual ($n/n_{\mathrm{crit}} \sim 100$) plasma, details which should motivate further study. We emphasize that ASE and SIB lack the observed θ, I, and polarization dependence, and STA the observed I dependence, and are weak as noted above.

VH with small $L \sim x_{\mathrm{osc}}$ must be distinguished from the nonlinear wave-breaking regime of RA [23] that occurs for $L \gg x_{\mathrm{osc}}$. The latter involves slow, many-cycle buildup of a resonant plasma wave and electric field at the critical surface which eventually break. For our extremely steep gradients, the buildup time is subcycle [24] and the critical surface field enhancement negligible [9], clearly placing the experiment in the regime discussed by Brunel. Thus we conclude that the extra absorption is indeed vacuum heating.

In summary, we report to our knowledge the first experimental identification of VH absorption as predicted in numerous theoretical studies [4–6]. Significant extensions should include correlations of VH with surface high harmonic generation [12] and two-color, phase-dependent measurements of VH [25] for both planar targets and nanoclusters.

This work was supported by Department of Energy Grant No. DEFG03-97-ER54439 and Robert Welch Foundation Grant No. F-1038.

*Electronic address: downer@physics.utexas.edu

[1] S. Backus *et al.*, Rev. Sci. Instrum. **69**, 1207 (1998).
[2] R. M. More *et al.*, J. Phys. (Paris), Colloq. **61**, C7-43 (1988).
[3] H. M. Milchberg and R. R. Freeman, Phys. Fluids B **2**, 1395 (1990); D. F. Price *et al.*, Phys. Rev. Lett. **75**, 252 (1995), and references therein.
[4] F. Brunel, Phys. Rev. Lett. **59**, 52 (1987); Phys. Fluids **31**, 2714 (1988).
[5] P. Gibbon and A. R. Bell, Phys. Rev. Lett. **68**, 1535 (1992); **73**, 664 (1994).
[6] H. Ruhl and P. Mulser, Phys. Lett. A **205**, 388 (1995); G. Bonnaud *et al.*, Laser Part. Beams **9**, 339 (1991); L. Cao, W. Chang, and Z. Yue, Phys. Plasmas **5**, 499 (1998); S. V. Bulanov *et al.*, Phys. Lett. A **195**, 84 (1994); S. Kato *et al.*, Phys. Fluids B **5**, 564 (1993).
[7] W. Rozmus *et al.*, Phys. Plasmas **3**, 360 (1996); R. Cauble and W. Rozmus, Phys. Rev. E **52**, 2974 (1995).
[8] E. S. Weibel, Phys. Fluids **10**, 741 (1967); A. A. Andreev *et al.*, Phys. Rev. E **58**, 2424 (1998).
[9] P. J. Catto and R. M. More, Phys. Fluids **20**, 704 (1977); T.-Y. Yang *et al.*, Phys. Plasmas **2**, 3146 (1995).
[10] T.-Y. Yang *et al.*, Phys. Plasmas **3**, 2702 (1996).
[11] M. M. Murnane *et al.*, Science **251**, 531 (1991).
[12] P. A. Norreys *et al.*, Phys. Rev. Lett. **76**, 1832 (1996), and references therein.
[13] T. Ditmire *et al.*, Nature (London) **386**, 54 (1997); T. Donnelly *et al.*, Phys. Rev. Lett. **76**, 2472 (1996).
[14] S. Jackel *et al.*, Opt. Lett. **20**, 1086 (1995); A. Rundquist *et al.*, Science **280**, 1412 (1998); S. V. Bulanov *et al.*, Phys. Lett. A **195**, 84 (1994).
[15] P. B. Corkum, Phys. Rev. Lett. **71**, 1994 (1993); A. L'Huillier and P. Balcou, Phys. Rev. Lett. **70**, 774 (1993).
[16] W. L. Kruer, *The Physics of Laser Plasma Interactions* (Addison-Wesley, New York, 1988).
[17] P. Blanc *et al.*, J. Opt. Soc. Am. B **13**, 118 (1996).
[18] W. M. Wood *et al.*, Opt. Lett. **13**, 984 (1988).
[19] M. K. Grimes, Ph.D. dissertation, University of Texas at Austin, 1998.
[20] S. Augst *et al.*, J. Opt. Soc. Am. B **8**, 858 (1991).
[21] Ya. B. Zeldovich and Yu. P. Raizer *Physics of Shock Waves and High-Temperature Hydrodynamic Phenomena* (Academic Press, New York, 1966), Chap. 1.
[22] H. M. Milchberg and R. R. Freeman, J. Opt. Soc. Am. B **6**, 1351 (1989).
[23] J. P. Friedberg *et al.*, Phys. Rev. Lett. **28**, 795 (1972).
[24] J. Albritton and P. Koch, Phys. Fluids **18**, 1136 (1975).
[25] D. W. Schumacher *et al.*, Phys. Rev. Lett. **73**, 1344 (1994).